

## Frequency-dependent AVA variations in thinly layered porous media

Lanfeng Liu<sup>1</sup>, Siyuan Cao<sup>1</sup>, Dehua Han<sup>2</sup>, Lu Wang<sup>3</sup>,

1. CNPC Key Laboratory of geophysical, University of petroleum, Beijing; 2. University of Houston;

3. Logging Instrument Plant of China Petroleum Logging CO.LTD, Xi an, Shanxi

### Summary

Amplitude-Versus-Offset (AVO) technology has successfully helped to detect hydrocarbon reservoir for more than two decades. However, the Zoeppritz equation only considers the elastic properties of the media, the non-elastic behaviors are ignored. There are still some problems that the traditional AVO technology doesn't handle adequately. Although the frequency-dependent AVO technology has been brought forward, a theory is lacking to guide it. Based on White's patchy saturation model, we have investigated characteristics of the frequency dependent Amplitude Versus incident-Angle (AVA) at an interface between a non-dispersive medium and a patchy-saturated dispersive medium. And then, numerical modeling based on Biot's poroelastic wave theory was performed on three selected reservoir models. The numerical modeling results confirmed our analytical analysis. These variations could provide insight for frequency-dependent AVO analysis.

### Introduction

For more than two decades, with the quick development in seismic exploration, AVO technology has achieved remarkable advancement and been extensively implemented in oil industry. However, the Zoeppritz equation only considers the elastic properties of the rocks. The non-elastic properties, such as velocity dispersion and attenuation, are ignored. There are still some problems that the traditional AVO technology doesn't handle adequately. For years, geophysicists have noticed low-frequency seismic anomalies associated with hydrocarbon reservoirs (Taner et al., 1979), and this topic is gaining more and more attention (Goloshubin et al., 2000; Castagna et al., 2003; Komeev et al., 2004; Chapman et al., 2006). Therefore, we should consider the effects of dispersion and attenuation on traditional AVO anomalies.

Although some researchers have done some significant attempts on the frequency-dependent AVO analysis (Yoo et al., 2005; Marmalyevskyy et al., 2006; Chapman et al., 2006; Odebeatu et al., 2006; Liu et al., 2006), a theory is still lacking to guide it. Based on patchy-saturated model, we try to investigate characteristics of the angle-dependent reflection coefficient as a function of frequency at an interface between a non-dispersive medium and a patchy-saturated dispersive medium and expect to provide some insights for frequency-dependent AVO analysis.

### Velocity dispersion and attenuation

For simplicity, we consider a periodic layered system composed of two porous media (1 and 2) with thickness  $d_l, l = 1, 2$  and period  $d_1 + d_2$ . Here  $d_1$  and  $d_2$  are much smaller than the seismic wavelength. The analytical solution for the periodic layered system yields the frequency-dependent P-wave phase velocity  $V_p$  and quality factor  $Q_p$  for a given set of rock properties (White et al., 1975; Carcione and Picotti, 2006).  $V_p$  and  $Q_p$  are given by

$$\frac{1}{Q_p} = \frac{\text{Im}(E)}{\text{Re}(E)} \quad (1)$$

$$V_p = \left[ \text{Re} \left( \frac{1}{V} \right) \right]^{-1} \quad (2)$$

Where

$$V = \sqrt{\frac{E}{\rho_b}} \quad (3)$$

$$E = \left[ \frac{1}{E_0} + \frac{2(r_2 - r_1)}{i\omega(d_1 + d_2)(I_1 + I_2)} \right]^{-1} \quad (4)$$

$$E_0 = \left( \frac{p_1}{E_{G1}} + \frac{p_2}{E_{G2}} \right)^{-1} ; \quad r = \frac{BM}{E_G} ;$$

$$I = \frac{\eta}{k\kappa} \coth \left( \frac{kd}{2} \right); \quad \rho_b = p_1\rho_{b1} + p_2\rho_{b2}$$

Here,  $E$  is the complex modulus for a P-wave traveling along the direction perpendicular to the layering, also called plane-wave modulus,  $\text{Re}(E)$  and  $\text{Im}(E)$  are the real and imaginary parts of the complex modulus;  $V$  is the complex velocity;  $\rho_b$  is the bulk density of porous layering;  $\rho_{b1}$  and  $\rho_{b2}$  are the density of porous media 1 and 2;  $p_s = d_s / (d_1 + d_2)$  with  $s = 1, 2$ ; Omitting the subscript  $s$ , we have for each media

$$E_G = K_{dry} + B^2M + \frac{4}{3}\mu_{dry} \quad (5)$$

### Frequency-dependent AVA variations in thinly layered porous media

$$M = \frac{K_m}{1 - K_{dry}/K_m + \phi(K_m/K_f - 1)} \quad (6)$$

Where,  $E_G$  is called Gaussmann modulus. Finally,  $k$  is the complex wavenumber of the slow P-wave velocity and is given by

$$k = \sqrt{\frac{i\omega\eta E_G}{\kappa M \left( K_{dry} + \frac{4}{3}\mu_{dry} \right)}} \quad (7)$$

The frequency-dependent S-wave phase velocity  $V_s$  and quality factor  $Q_s$  for the periodic layered system can be calculated by Biot's analytical solutions as follows

$$\frac{1}{Q_s} = \frac{\frac{\gamma_3}{\omega} \gamma_1^2}{\gamma_2^2 - \gamma_1^2 \gamma_2 + \left( \frac{\gamma_3}{\omega} \right)^2} \quad (8)$$

$$V_s = \sqrt{\frac{\mu}{\rho_b} \frac{\gamma_2^2 + \left( \frac{\gamma_3}{\omega} \right)^2}{\gamma_2^2 - \gamma_1^2 \gamma_2 + \left( \frac{\gamma_3}{\omega} \right)^2}} \quad (9)$$

Where  $\gamma_1 = \frac{\rho_f}{\rho_b}$ ,  $\gamma_2 = \frac{M}{\rho_b}$ ,  $\gamma_3 = \frac{\eta/\kappa}{\rho_b}$  are three elastic moduli.

#### Frequency-dependent Amplitude versus Incident Angle

To systematically investigate dispersion effects on the magnitude and phase angle of angle-dependent reflection coefficients, we select three reservoir models that represent three types of reservoirs commonly encountered in oil exploration. The overburden shale, rock-frame, and pore-fluid properties of models 1, 2 and 3 are same as [Ren et al. 2009](#). For each model, the reservoir consists of 1-m thick layers with the same rock frame, but brine-saturated layers alternate with gas-saturated layers. Although the stratified model might not be realistic physically, it does represent the attenuation associated with White's patchy-saturation model ([Dutta and Seriff, 1979](#)). Moreover, the stratified layering simplified the numerical modeling.

Because of velocity dispersion and attenuation of P-wave and S-wave, reflection coefficients from the interface between the non-dispersive overburden and dispersive reservoir rock are a function of frequency ( $\omega$ ). The angle-

incident P-wave reflection coefficient ( $R_{pp}(\omega)$ ) can be calculated through solving the linear equations 10, which can be deduced from [Trapeznikova, 1985](#).

$$\begin{pmatrix} \sin\theta_{p1} & \cos\theta_{s1} & -\sin\theta_{p2} & \cos\theta_{s2} \\ \cos\theta_{p1} & -\sin\theta_{s1} & \cos\theta_{p2} & \sin\theta_{s2} \\ \frac{\rho_1 c_{s1}^2}{c_{p1}} \sin 2\theta_{p1} & \rho_1 c_{s1} \cos 2\theta_{s1} & \frac{\rho_2 c_{s2}^2}{c_{p2}} \sin 2\theta_{p2} & -\rho_2 c_{s2} \cos 2\theta_{s2} \\ \rho_1 c_{p1} \cos 2\theta_{s1} & -\rho_1 c_{s1} \sin 2\theta_{s1} & -\rho_2 c_{p2} \cos 2\theta_{s2} & -\rho_2 c_{s2} \sin 2\theta_{s2} \end{pmatrix} \times \begin{pmatrix} R_{pp} \\ R_{ps} \\ T_{pp} \\ T_{ps} \end{pmatrix} = \begin{pmatrix} -\sin\theta_{p1} \\ \cos\theta_{p1} \\ \frac{\rho_1 c_{s1}^2}{c_{p1}} \sin 2\theta_{p1} \\ -\rho_1 c_{p1} \cos 2\theta_{s1} \end{pmatrix} \quad (10)$$

Where,  $c$  is a frequency-dependent modulus, subscriptions  $p$  and  $s$  represent the compressional and shear wave; subscriptions 1 and 2 represent upper nondispersive overburden shale and lower dispersive sand reservoir, respectively. Omitting the subscriptions, we have  $\frac{1}{c} = \frac{1}{V} - \frac{i\alpha}{\omega}$ , Here,  $V$  and  $\alpha$  are phase velocity and attenuation, and  $\alpha = \left( \sqrt{Q^2 + 1} - Q \right) \frac{\omega}{V}$  ([Carcione, 2001](#)).

$\theta_{p1}$  is the P-wave incident angle, and it is equal to the P-wave reflected angle;  $\theta_{s1}$  is the reflected angle of the S-wave;  $\theta_{p2}$  and  $\theta_{s2}$  are the angles of transmitted P- and S-wave, respectively; and have

$$\theta_{s1} = \arcsin \frac{\sin\theta_{p1} (i\omega/V_{p1} + \alpha_{p1})}{i\omega/V_{s1} + \alpha_{s1}},$$

$$\theta_{p2} = \arcsin \frac{\sin\theta_{p1} (i\omega/V_{p1} + \alpha_{p1})}{i\omega/V_{p2} + \alpha_{p2}},$$

$$\theta_{s2} = \arcsin \frac{\sin\theta_{p1} (i\omega/V_{p1} + \alpha_{p1})}{i\omega/V_{s2} + \alpha_{s2}}.$$

The phase velocities of P- ( $V_p$ ) and S-wave ( $V_s$ ) in the stratified reservoir sands are computed based on equations 2 and 9, respectively, and plotted as a function of frequency for models 1, 2 and 3 in Figure 1a. The reciprocal of the

## Frequency-dependent AVA variations in thinly layered porous media

quality factors of P- ( $1/Q_p$ ) and S-wave ( $1/Q_s$ ) in the stratified reservoir sands are calculated by equations 1 and 8, respectively and plotted as a function of frequency for models 1, 2 and 3 in Figure 1b.

The phase velocities and attenuations from equations 1, 2, 8 and 9 are inserted to linear equation 10, then the P-wave reflection coefficient ( $R_{pp}(\omega)$ ) at different incident-angles can be computed. The reflection magnitude and phase angle are derived by  $R_{pp}(\omega)$

$$\text{and } \psi(\omega) = \tan^{-1} \left( \frac{\text{Im}(R_{pp}(\omega))}{\text{Re}(R_{pp}(\omega))} \right), \text{ respectively.}$$

The magnitude and phase angle of P-wave reflection coefficient are plotted as a function of incident angle and frequency in Figure 2a, 2b for model 1, Figure 3a, 3b for model 2, and Figure 4a, 4b for model 3, respectively.

For model 1, the reservoir is consolidated sand, and the porosity and permeability are small. The P-wave velocity dispersion and attenuation are also small. Its acoustic impedance is larger than that of the overlying shale. In the amplitude versus incident-angle domain, Figure 2a shows that the reflection magnitude decreases with increasing incident angle, which agrees with traditional Class I AVO response. In the amplitude versus frequency domain, Figure 2a shows that when the incident-angle is less than 30°, the reflection magnitude increases toward higher frequencies. This observation coincides with the low-frequency dim-out response presented by [Ren and his coauthors \(2009\)](#). For this particular reservoir model, the reflection becomes more complex when the incident-angle passes 30°. First, the reflection magnitude becomes very small. Second, the phase polarity is reversed from positive to negative. Third, because of the phase reversal, reflection magnitude decreases when frequency increases as shown in Figure 2a at 40° incident-angle. Figure 2b indicated an obvious phase reversal at incident angle of about 33°.

For model 2, the reservoir is mid-consolidated sand and the porosity and permeability are moderate. The P-wave velocity dispersion and attenuation are larger than that of the model 1 reservoir. Its acoustic impedance is slightly smaller than that of the overlying shale. It is shown in Figure 3, when frequency is less than 36Hz, the phase angles are negative, and the reflection magnitude increases with increasing incident angle. When frequency exceeds 36Hz, the phase angles change from positive to negative as incident-angle increases, and the reflection magnitude increases in general. Figure 3 also shows that the reflection magnitude increases toward lower-frequency and also

shows a phase reversal from negative to positive when frequency increases from low to high. These observations coincide with the frequency-domain phase-reversal reservoir showed by [Ren et al \(2009\)](#).

For model 3, the reservoir is shallow unconsolidated sand and the porosity and permeability are very large. The P-wave velocity dispersion and attenuation are also significant. Its acoustic impedance is smaller than that of the overlying shale. Figure 4a shows that in general of the reflection magnitude increases with increasing incidence-angle. This variation agrees with the response of traditional AVO class III. In the amplitude versus frequency domain, the reflection magnitude increases toward lower-frequencies. It coincides with the low-frequency bright-spot reservoir in [Ren et al., 2009](#). Figure 4b illustrates that the phase angles are all negative and become smaller with incident angle increases.

### Wave-propagation numerical modeling

We performed wave-propagation numerical modeling on the three reservoir models to demonstrate velocity dispersion and attenuation effects on seismic amplitudes in porous media. We generated synthetic traces for porous layered media using the OASES software package. Developed by [Schmidt and Tango \(1986\)](#), OASES was adopted for the Biot's poroelastic model by [Stern et al. \(1985\)](#). [Stern et al. \(1985\)](#) and [Schmidt \(2004\)](#) have a detail description for this package.

In each model, the total reservoir thickness is 200 m. It is a seismically thick reservoir such that the reflection from the base of the reservoir does not interfere with the reflection from the top. Half-spaces above and below the reservoir are shale with the same properties. Source and receiver are 950 m and 1000 m, respectively, above the top of the reservoir.

For each of the three reservoir models, impulse response from the OASES program were convolved with 15-,20-,25-,30-,35-,40-,45-,50-,55-Hz Ricker wavelets. The reflection magnitude from the top interface of reservoir models are plotted as a function of frequency and offset in Figure 5a, b and c for model 1, 2 and 3, respectively.

For model 1, figure 5a shows that when the offset is smaller than 1000m, the reflection magnitude increases from lower to higher frequencies; however, when the offset is larger than 1400m, the magnitude decreases as frequency increases. For model 2 and 3, Figure 5b and 5c illustrate that the reflection magnitude increases with increasing offset, and in amplitude versus frequency domain, the reflection magnitude decreases as frequency increases. In general, the results from the numerical modeling agree with the analytic predictions.

## Frequency-dependent AVA variations in thinly layered porous media

### Conclusions

In this paper, we studied characteristics of the magnitude and phase angle of P-wave incident-angle dependent reflection coefficient from an interface between a non-dispersive medium and a dispersive medium. Moreover, we performed numerical modeling for three representative reservoir models by using Biot's poroelastic wave theory.

According to the results of our study, we have the following observations for the frequency and incident-angle dependent reflection responses. First, for acoustically hard rock, at normal incidence and smaller incident angles, the reflection magnitude increases when frequency increases; while in the amplitude-versus-offset domain, it follows the traditional AVO class I response, amplitude decreases with increasing offsets. Second, for acoustically hard and slightly harder rocks, in the amplitude-versus-frequency domain, phase reversal may present when frequency increases from low to high. This type of response can happen in traditional AVO class I and II reservoirs, but the phase reversal will be in different incident-angle ranges. Third, for acoustically soft reservoirs, in amplitude-versus-offset domain, the reflection magnitude increases with offset similar to AVO class III responses, however in amplitude-versus-frequency domain, the reflection magnitude increases when frequency decreases, which appears in all the frequencies we have investigated.

### Acknowledgments

We extremely appreciate Dr. Haitao Ren's instructive guidance and other helps that he provided for this work. We would like to thank the Department of Ocean Engineering at the Massachusetts Institute of Technology for permission to use the OASES software package.

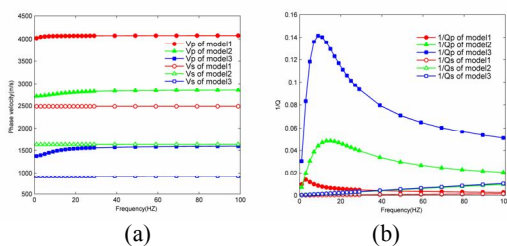


Figure 1: (a) Phase velocity and (b) reciprocal of the quality factor versus frequency for reservoir model 1 (circle), 2 (triangle), and 3 (square), solid represents compressional wave and hollow represents shear wave

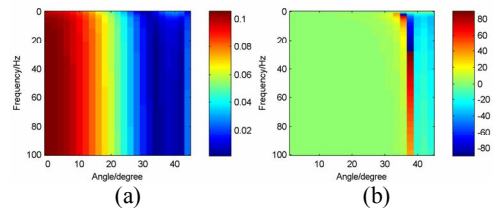


Figure 2: (a) Magnitude, and (b) phase angle, of the angle-incident reflection coefficient versus frequency for reservoir model 1

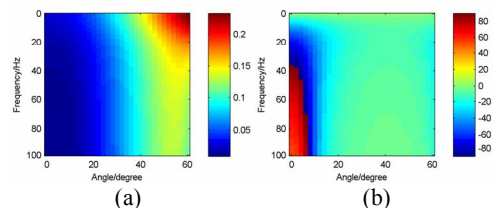


Figure 3: (a) Magnitude, and (b) phase angle, of the angle-incident reflection coefficient versus frequency for reservoir model 2

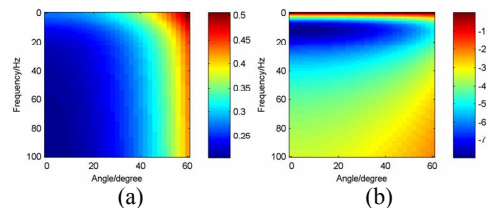


Figure 4: (a) Magnitude, and (b) phase angle, of the angle-incident reflection coefficient versus frequency for reservoir model 3

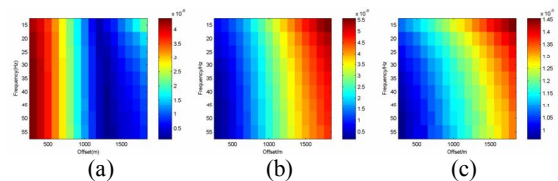


Figure 5: Reflection magnitude from the top interface versus frequency and offset for (a) model 1, (b) model 2, and (c) model 3.

**EDITED REFERENCES**

Note: This reference list is a copy-edited version of the reference list submitted by the author. Reference lists for the 2010 SEG Technical Program Expanded Abstracts have been copy edited so that references provided with the online metadata for each paper will achieve a high degree of linking to cited sources that appear on the Web.

**REFERENCES**

- Carcione, J. M., 2001, Wave fields in real media: Wave propagation in an isotropic, anelastic and porous media: Pergamon Press.
- Carcione, J. M., and S. Picotti, 2006, P-wave seismic attenuation by slow-wave diffusion: Effects of inhomogeneous rock properties: *Geophysics*, **71**, no. 3, O1–O8, [doi:10.1190/1.2194512](https://doi.org/10.1190/1.2194512).
- Castagna, J. P., S. Sun, and R. W. Seigfried, 2003, Instantaneous spectral analysis: Detection of low-frequency shadows associated with hydrocarbons: *The Leading Edge*, **22**, no. 2, 120–127, [doi:10.1190/1.1559038](https://doi.org/10.1190/1.1559038).
- Chapman, M., E. Liu, and X. Li, 2006, The influence of fluid-sensitive dispersion and attenuation on AVO analysis: *Geophysical Journal International*, **167**, no. 1, 89–105, [doi:10.1111/j.1365-246X.2006.02919.x](https://doi.org/10.1111/j.1365-246X.2006.02919.x).
- Dutta, N. C., and A. J. Seriff, 1979, On White's model of attenuation in rocks with partial saturation: *Geophysics*, **44**, 1806–1812, [doi:10.1190/1.1440940](https://doi.org/10.1190/1.1440940).
- Goloshubin, G. M., and V. A. Korneev, 2000, Seismic low-frequency effects from fluid-saturated reservoir: 70th Annual International Meeting, SEG, Expanded Abstracts, 976–979.
- Ren, H., G. Goloshubin, and F. J. Hilterman, 2009, Poroelastic analysis of amplitude versus frequency variations: *Geophysics*, **74**, no. 6, N41, [doi:10.1190/1.3207863](https://doi.org/10.1190/1.3207863).
- Korneev, V. A., G. M. Goloshubin, T. M. Daley, and D. B. Silin, 2004, Seismic low-frequency effects in monitoring fluid-saturated reservoirs: *Geophysics*, **69**, 522–532, [doi:10.1190/1.1707072](https://doi.org/10.1190/1.1707072).
- Liu, E., M. Chapman, N. Loizou, and X. Li, 2006, Applications of spectral decomposition for AVO analyses in the west of Shetland: 76th Annual International Meeting, SEG, Expanded Abstracts, 279–283.
- Marmalyevskyy, N., Roganov Y., 2006, Frequency depending AVO for a gas-saturated periodical thin-layered stack: 76th Annual International Meeting, SEG, Expanded Abstracts, 274–278.
- Odebeatu, E., J. Zhang, M. Chapman, E. Liu and X. Y. Li, 2006, Application of spectral decomposition to detection of dispersion anomalies associated with gas saturation: *The Leading Edge*, **25**, no. 2, 206–210, [doi:10.1190/1.2172314](https://doi.org/10.1190/1.2172314).
- Schmidt, H., and G. Tango, 1986, Efficient global matrix approach to the computation of synthetic seismograms: *Geophysical Journal of the Royal Astronomical Society*, **84**, 331–359.
- Schmidt, H., 2004, OASES Version 3.1 user guide and reference manual: Massachusetts Institute of Technology.
- Stern, M., A. Bedford, and H. R. Millwater, 1985, Wave reflection from a sediment layer with depth-dependent properties: *The Journal of the Acoustical Society of America*, **77**, no. 5, 1781–1788, [doi:10.1121/1.391927](https://doi.org/10.1121/1.391927).
- Taner, M. T., F. Koehler, and E. Sheriff, 1979, Complex seismic trace analysis: *Geophysics*, **44**, 1041–1063, [doi:10.1190/1.1440994](https://doi.org/10.1190/1.1440994).

Trapeznikova, N. A., 1985, Prognosis and interpretation of seismic wave dynamics: Nauka, Moscow, 115.

White, J. E., N. G. Mikhaylova, and F. M. Lyakhovitskiy, 1975, Low-frequency seismic waves in fluid saturated layered rocks: Izvestiya, Academy of Sciences, USSR. Physics of the Solid Earth, **11**, 654–659.

Yoo, S., Gibson R L., 2005, Frequency dependent AVO analysis after target oriented stretch correction: 75th Annual International Meeting, SEG, Expanded Abstracts, 293-296.